BIOCHEMISTRY
including biophysical chemistry & molecular biology

Article

pubs.acs.org/biochemistry

Effects of Desialylation on Human α1-Acid Glycoprotein−Ligand Interactions

Richard Y.-C. Huang[†,‡] and Jeffrey W. Hudgens*[,†,‡]

[†]Bioprocess Measurements Group, Biomolecular Measurement Division, National Institute of Standards and Technology, Gaithersburg, Maryland 20899, United States

[‡]Institute for Bioscience and Biotechnology Research, Rockville, Maryland 20850, United States

Supporting Information

ABSTRACT: Human α1-acid glycoprotein (AGP), an acute-phase glycoprotein, exists predominantly in blood. With its ability to bind basic, lipophilic, and acidic drugs, AGP has served as a drug carrier. It has been shown that the carbohydrate composition of AGP changes in response to tissue injury, inflammation, or infection and can have a great impact on AGP's drug binding activities. The molecular-level details of the effects of desialylation on the AGP conformation and AGP−ligand interactions, however, are unknown. Here we report the use of hydrogen−deuterium exchange coupled with mass spectrometry (HDX−MS) to reveal the changes in AGP conformational dynamics induced by the removal of terminal sialic acid. HDX−MS also reveals the changes in the conformational dynamics of sialylated and unsialylated AGP upon formation of complexes of holo-AGP with progesterone or propranolol. Our HDX−MS results demonstrate that desialylation stabilizes two loop regions that are exterior to the β-sheet barrel in AGP, and this stabilization minimizes the conformational changes of AGP upon binding with progesterone or propranolol.

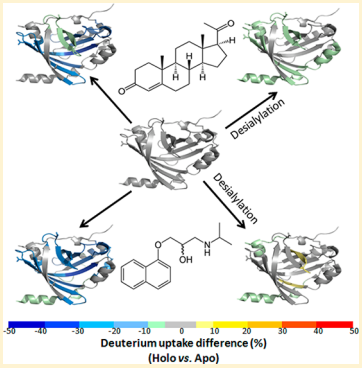

The influence of glycan structure on protein biophysical properties is the overarching theme of this study of human α1-acid glycoprotein (AGP), which is a 183-residue, 40 kDa protein. AGP, also known as orosomucoid, is one of the positive acute-phase proteins, as its plasma concentration increases in response to inflammation. AGP consists of an eight-stranded β-barrel (β-strands A−H) surrounded by three helices and four loop regions (loops I−IV)[1] (Figure 1). AGP has two disulfide bonds,[2] and its five N-linked complex-type glycans comprise nearly 45% of the total molecular weight.[3] The β-barrel of AGP forms a ligand binding cavity that can bind to basic, lipophilic, and acidic small molecules.[4] This property makes AGP an important drug-binding protein in human plasma.[1,4,5]

Over the past 34 years, investigators have discovered that glycosylation in AGP affects physiologic response. The proliferative response of lymphocytes can be suppressed by AGP glycans.[6] The heterogeneity of AGP glycoforms depends strongly on the pathophysiological conditions of the blood plasma donor.[7] The drug binding capacity of AGP varies with different types of branching of its glycan chains.[8] The immunomodulatory and drug binding activities of AGP show a strong dependence on carbohydrate composition and concentration.[9] Desialylation of AGP can inhibit the aggregation of platelets in blood, and desialylation can also affect AGP drug binding.[9,10] These observations stimulated our interest in the identification of direct mechanisms of desialylation-induced changes in AGP conformational dynamics and ligand binding activities, as such correlations are unknown.

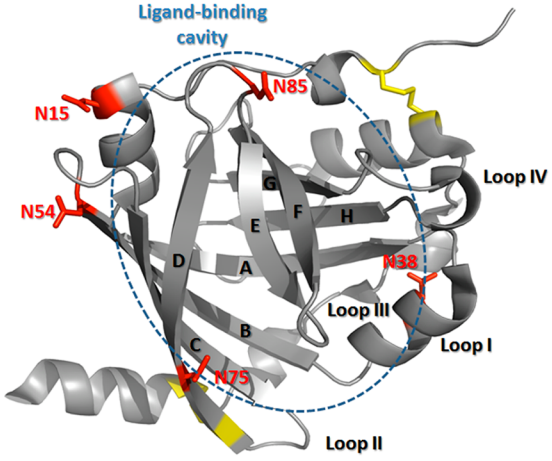

Figure 1. Structure of unglycosylated AGP. The X-ray crystal structure of unglycosylated AGP (PDB entry 3KQ0)[1] shows five N-linked glycosylation sites (red, Asn) and two disulfide bonds (yellow) together with an eight-stranded β-barrel (β-strands A−H) and four loop regions (loops I−IV). The ligand-binding cavity is encircled.

Hydrogen−deuterium exchange coupled with mass spectrometry (HDX−MS)[11−18] is a powerful tool for conducting measurements of the relative rates of exchange between amide hydrogens and deuteriums in D_2O solutions. The experimental

Received: March 8, 2013
Published: September 16, 2013

outcome provides inferences on the stability of hydrogen bonding, which are inversely related to relative solvent exchange rates. This strategy allows us to measure changes in protein conformational flexibility (changes in hydrogen bonding) along the entire protein backbone (except at proline) that are caused by a change in ligand binding or a change of the external environment.

Only a few studies have employed HDX to investigate the effects of glycosylation upon protein structure. The earliest investigators used HDX with nuclear magnetic resonance (NMR) to observe differences between native bovine glycosylated RNase B and unglycosylated RNase A[19] and native, GlcNAc-derived, and unglycosylated human chorionic gonadotropin.[20] HDX−MS measurements have facilitated comparisons between the dynamical structures of native glycosylated and unglycosylated IgG1[21,22] and human serpin α1-antitrypsin.[23]

In this study, we aimed to address two important issues with respect to the effects of desialylation on the AGP biophysical properties. First, using HDX−MS, we measured the changes in the conformational dynamics of AGP that are induced by the removal of the terminal sialic acid groups from the native AGP glycans. Second, by monitoring the differential changes in the HDX behavior of holo-AGP that forms through complexation with progesterone or propranolol, we measured the changes in AGP−ligand interactions for sialylated and unsialylated AGP. To help clarify the effects of glycan structure upon each measured HDX−MS profile, we have comprehensively characterized the distribution of glycan structures occupying each glycosite of the AGP glycoform samples. During this work, we employed electron-transfer dissociation during tandem mass spectrometry experiments to determine the time-resolved, D uptake of each glycan structure.

EXPERIMENTAL PROCEDURES

Reagents and Materials. Human α1-acid glycoprotein, propranolol hydrochloride, progesterone, sodium phosphate dihydrate, sodium phosphate monohydrate, porcine pepsin, citric acid, sodium citrate, sodium chloride, sodium sulfate, sodium cyanoborohydride, ethanolamine, and an α-1(2,3,4)-fucosidase solution were purchased from Sigma-Aldrich (St. Louis, MO). α-2(3,6,8)-Neuraminidase and peptide:*N*-glycosidase (PNGase F) were from New England Biolabs (Ipswich, MA). The synthetic peptide, HHHHHHIIKIIK, was purchased from Genscript (Piscataway, NJ). D_2O was from Cambridge Isotope Laboratories Inc. (Andover, MA). Tris(2-carboxyethyl)phosphine hydrochloride (TCEP-HCl) and high-purity guanidine hydrochloride (GdmCl) were from Thermo Scientific (Rockford, IL).

Preparation of Desialylated/Defucosylated AGP. The desialylated/defucosylated AGP was prepared through incubation of 500 μg of native AGP with 20 milliunits of α-2(3,6,8)-neuraminidase and 1 milliunit of α-1(2,3,4)-fucosidase in the presence of 1 μg of BSA in 250 mmol/L sodium phosphate buffer (pH 5.0) for (20 ± 2) h at 37 °C. Native AGP (500 μg) was incubated in 500 mmol/L sodium phosphate buffer (pH 7.5) for (20 ± 2) h at 37 °C. AGP samples were purified by size exclusion chromatography using a Superdex 10 mm × 300 mm S200 column (GE Healthcare, Wauwatosa, WI) operated under an isocratic flow at a rate of 0.5 mL/min with PBS buffer [10 mmol/L sodium phosphate and 138 mmol/L NaCl (pH 7.4)]. The purified samples were collected at >10% peak height and concentrated using a 10 kDa molecular mass cutoff Amicon concentrator (Millipore, Billerica, MA). The concentration of the final protein solution was measured by the BCA protein assay following the manufacturer's protocol (Thermo Fisher, Rockford, IL). The protein solution was aliquoted and stored at −80 °C.

Mass Spectrometry Analyses of Glycoproteins and Glycopeptides. The masses of glycosylated AGP variants were verified using matrix-assisted laser desorption ionization (MALDI). The protein solution was mixed in a 1:1 ratio with 10 mg/mL sinapic acid (Sigma-Aldrich) in 50% acetonitrile and 0.1% formic acid (all chemical percentages reported as percent by volume). MALDI analyses were performed with an ABI 4700 Proteomics Analyzer (Applied Biosystems, Framingham, MA) equipped with an Nd:YAG laser (355 nm, 3−7 ns pulses). The instrument was operated in linear, positive ion mode with an acceleration voltage of 40 kV. Spectra were averaged from 1000 laser shots at 200 Hz for each spot.

Peptic peptides of AGP were generated by passing 100 pmol of protein through an online pepsin digestion device containing immobilized pepsin in a 2 mm (diameter) × 2 cm (length) guard column (Upchurch Scientific, Oak Harbor, WA), which was prepared as described previously.[24] The peptide solution was collected at a flow rate of 200 μL/min, with 0.1% TFA, desalted using NuTip C-18 (Glygen, Columbia, MD), lyophilized, and resuspended in 10 μL of water. The glycopeptides of each sample were enriched with a Novagen ProteoExtract Glycopeptide Enrichment Kit (Millipore) following the manufacturer's protocol. Glycopeptides were separated with an Eclipse Plus C18 analytical column [2.1 mm (diameter) × 10 cm (length) (Agilent, Santa Clara, CA)] via an Agilent 1200 HPLC system with a 30 min gradient operated at a flow rate of 200 μL/min and analyzed on a Thermo LTQ Orbitrap Discovery (Thermo Fisher, San Jose, CA). Solvent A of the HPLC system was water containing 0.1% formic acid, and solvent B was 80% acetonitrile and 20% water containing 0.1% formic acid. The gradient settings were as follows: 5 to 10% solvent B for 3 min, 10 to 45% solvent B for 25 min, 45 to 100% solvent B for 1 min, isocratic flow at 100% solvent B for 1 min, and then a return to 5% solvent B for 0.5 min. The following mass spectrometer settings were used: spray voltage, 4 kV; sheath gas flow rate, 35 (arbitrary units); capillary temperature, 250 °C; capillary voltage, 40 V; and tube lens, 200 V. The six most abundant precursor ions (other than singly charged ions) were activated by collision-induced dissociation (CID) and resolved by mass spectrometry for sequencing; this procedure defines our MS/MS method. The peaks observed in the product ion spectra (MS/MS) were centroided for each peptide during the acquisition.

Glycan Structure Determinations. Glycopeptides were first identified by analyzing MS/MS results of unglycosylated AGP (PNGaseF-treated) using the MassMatrix database search engine (http://www.massmatrix.net).[25,26] The following database search settings were used: enzyme, nonspecific; variable modification, deglycosylation of N; precursor ion tolerance, 10 ppm; product ion tolerance, 0.8 Da; maximal number of PTM per peptide, 2; minimal peptide length, 6 amino acids; maximal peptide length, 40 amino acids; minimal pp score, 5.0; maximal number of matches per spectrum, 1; and maximal number of combinations per match, 1. All identifications of peptides were manually confirmed. Given that CID fragmentation of an N-linked glycopeptide produces an intense [peptide + GlcNAc] ion, a mass list of each peptide with addition of one GlcNAc was generated and used to identify corresponding glycopep-

Table 1. Glycopeptides Used in HDX Analysis[a]

glycopeptide	glycosite	glycan structure	retention time (min)	observed mass	theoretical mass	mass error (ppm)	abundance (%)
			Native AGP				
VPVPITNATL	15	[HexNAc]4[Hex]5[NeuAc]2	3.5	3228.3738	3228.3683	1.7	61
FRNEEYNKSVQEIQ	38	[HexNAc]4[Hex]5[NeuAc]2	3.1	3987.6291	3987.6255	0.9	56
YFTPNKTEDTIF	54	[HexNAc]6[Hex]7[NeuAc]2	4.2	4409.7324	4409.7343	0.4	56
IYNTTYL	75	[HexNAc]5[Hex]6[NeuAc]3	1.1	3747.4515	3747.4431	2.2	81
NVQRENGTISRYVGGQEHFAHL	85	[HexNAc]6[Hex]7[NeuAc]4	3.9	6028.4704	6028.4638	1.1	95
			Desialylated AGP				
VPVPITNATL	15	[HexNAc]4[Hex]5	3.6	2646.175	2646.1775	0.9	95
FRNEEYNKSVQEIQ	38	[HexNAc]4[Hex]5	3.2	3405.4446	3405.4347	7.9	49
YFTPNKTEDTIF	54	[HexNAc]6[Hex]7	4.2	3827.5503	3827.5435	1.8	64
IYNTTYL	75	[HexNAc]5[Hex]6	1.2	2874.1548	2874.1569	0.7	≈100
NVQRENGTISRYVGGQEHFAHL	85	[HexNAc]6[Hex]7	3.8	4864.0892	4864.0822	1.4	≈100

[a]The most abundant glycopeptides identified in the two AGP variants were used in the HDX analysis. The compositions of glycans together with their observed glycopeptide masses and abundance (relative to other glycan forms identified at the corresponding glycosite) are listed ([HexNAc], GlcNAc; [Hex], mannose or galactose; and [NeuAc], sialic acid). A mass error (mass difference between observed mass and theoretical mass) of <10 ppm is considered accurate.

tides in the MS/MS spectra of AGP variants. The glycan structure of each glycopeptide was reconstructed by analyzing the MS/MS fragments (Figure S1 of the Supporting Information) and subsequently confirmed with an accurate mass measurement (<10 ppm).

Calculation of Glycan Distributions. The abundance of each glycan structure on the AGP variants was quantified using a label-free strategy. The corresponding LC peak area of each glycopeptide identified in the crude AGP samples was normalized to the total peak area of the glycopeptides presented at each glycosite. Three LC–MS runs of pepsin-digested AGP variants were applied with this strategy separately, and the results were averaged and reported with their standard deviations (1σ) (Table S1 of the Supporting Information).

HDX–MS. The ligand-free AGP (apo) samples were prepared by diluting the AGP glycovariants in PBS buffer [10 mmol/L sodium phosphate and 138 mmol/L NaCl (pH 7.4)] to prepare a 10 μmol/L final analytical concentration and equilibrated at 4 °C for 2 h. The AGP–progesterone and AGP–propranolol complexes (holo) were prepared by mixing AGP in a 1:2 ratio with progesterone and propranolol separately at a final protein concentration of 10 μmol/L in PBS buffer and equilibrated at 4 °C for 2 h.

HDX was conducted on an HDX PAL robot (LEAP Technologies, Carrboro, NC). The protein solution (5 μL) was diluted into 21 μL of D_2O buffer [20 mmol/L sodium phosphate and 500 mmol/L NaCl (pD 7.6)] at 3 °C. At selected times (30 s, 2 min, 5 min, 20 min, 40 min, and 60 min), HDX was quenched by mixing the sample with 30 μL of 500 mmol/L TCEP-HCl and 4 mol/L GdmHCl in 200 mmol/L sodium phosphate buffer (pH 2.5) at 1 °C. The quenched solution was injected into an online pepsin digestion device for 3 min. The digested protein solution was trapped on a C18 guard column [1.0 mm diameter, 5 μm (Grace Discovery Sciences)]. The peptide mixture was separated with a C18 analytical column [1.0 mm (diameter) × 5 cm (length), 1.9 μm, Hypersil GOLD (Thermo Scientific)] via a Dionex Ultimate 3000 UPLC system with a 9.5 min gradient operated with a binary mixture of solvents A and B at a flow rate of 50 μL/min. The following gradient settings were used: 5 to 35% solvent B for 3 min, 35 to 70% solvent B for 5 min, 70 to 100% solvent B for 0.5 min, isocratic flow at 100% solvent B for 0.5 min, and then a return to 5% solvent B for 0.5 min. Solvent A was water containing 0.1% formic acid, and solvent B was 80% acetonitrile and 20% water containing 0.1% formic acid. All LC connection lines and valves were housed in the refrigerated compartment of the HDX PAL at 2 °C. Peptides were analyzed on a Thermo LTQ Orbitrap Elite instrument (Thermo Fisher). The following instrument settings were used: spray voltage, 3.7 kV; sheath gas flow rate, 25 (arbitrary units); and capillary temperature, 270 °C. Three replicates were obtained for each on-exchange time point.

In the Orbitrap stage, spectra were acquired with the resolution set at 60000, which has been shown to yield accurate measurements of hydrogen and deuterium composition, presumably because the FTMS spectra do not suffer distortions of the destructive interference of isotopic envelope measurements as observed at higher resolution in FTMS.[27] Three biological replicates were obtained for each on-exchange time point.

HDX–ETD Measurements of the Uptake of Deuterium by Glycans. Prior to conducting HDX–ETD measurements on AGP, we used a synthetic peptide, HHHHHHIIKIIK, to monitor the extent of hydrogen scrambling, as described previously by Jørgensen and co-workers.[28] Briefly, 100 μmol/L synthetic peptide was prepared in D_2O and kept at 4 °C overnight to allow complete deuterium exchange. The solution was diluted 50-fold with cold H_2O buffer [50% MeOH and 0.5 mol/L acetic acid (pH 2.5)] and frozen on dry ice to quench the exchange reaction. When needed for analysis, the peptide solution was manually thawed and infused into the ESI source via a precooled 500 μL syringe (Hamilton, Reno, NV) operated at a flow rate of 50 μL/min. Using previously described methods,[28] the average extent of hydrogen scrambling, as computed from the c_i fragment ions, was (6.4 ± 0.2)% (Figure S2 of the Supporting Information) under mild instrumental conditions: capillary temperature, 100 °C; S lens, 50 V;

dx.doi.org/10.1021/bi4011094 | Biochemistry 2013, 52, 7127–7136

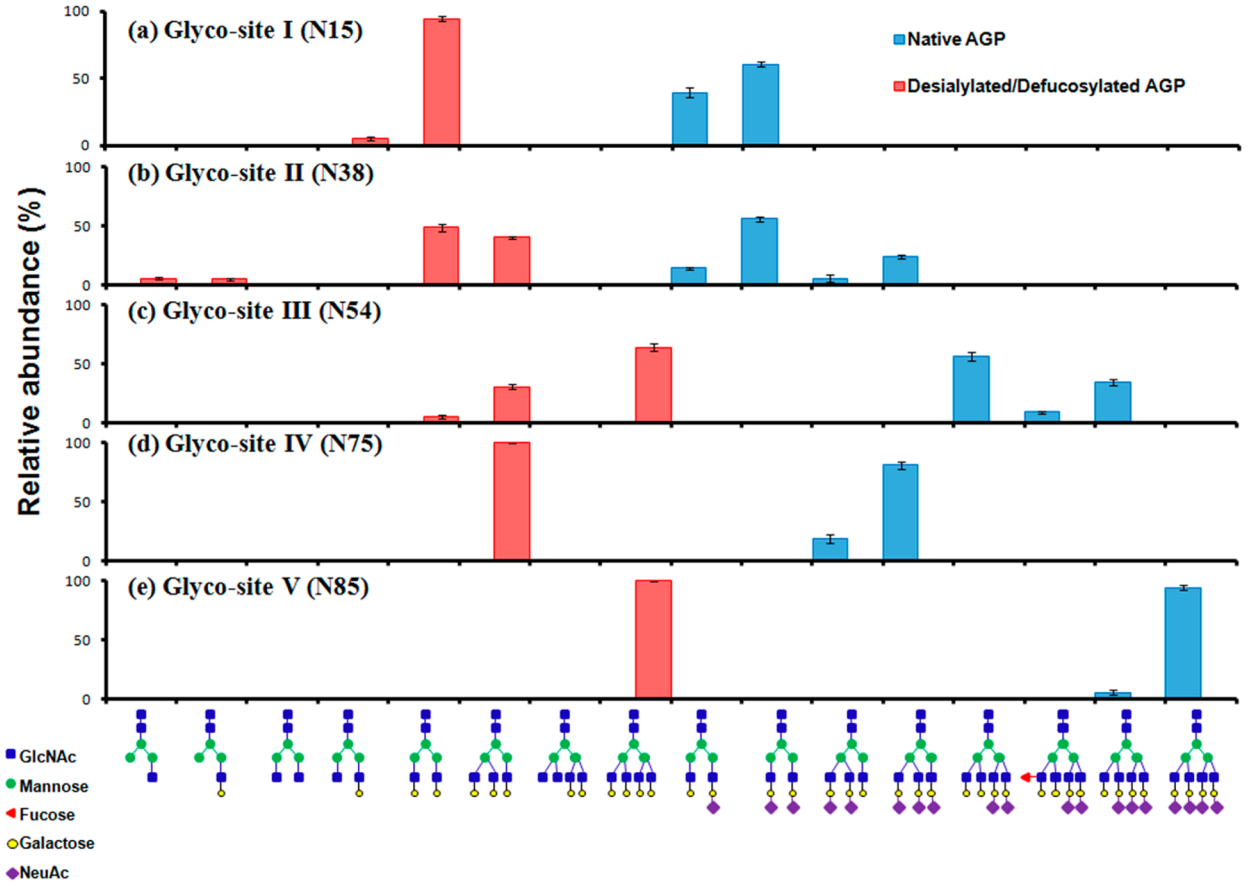

Figure 2. Distribution of glycan structures of AGP variants. The glycan structures identified at the five glycosites (a–e) of AGP variants by LC–MS/MS and their relative abundances are plotted on the *x*-axis, according to their complexity, from simple (left) to the most complex, sialylated, tetra-antennary glycan (right). The desialylated glycan distribution is somewhat simpler, as is seen by comparison of native AGP (blue) and desialylated/defucosylated AGP (red). Each bar represents an average of three trials reported with their standard deviation (1σ).

isolation width, 18 units; and ETD activation time, 300 ms on a Thermo LTQ Orbitrap Elite instrument coupled with an ETD source. (In this paper, the indicated measurement uncertainties are 1σ.) These conditions were applied during all HDX–ETD experiments.

For the HDX–ETD experiments on AGP, all procedures prior to ETD fragmentation were the same as for peptide-level HDX. Various precursor mass lists for ETD fragmentation were generated on the basis of the centroid m/z of the deuterated glycopeptides, ^{9}VPVPITNATL^{18}, ^{32}FRNEEYNKSVQEIQ^{45}, ^{50}YFTPNKTEDTIF^{61}, and ^{80}NVQRENGTISRYVGGQEHFAHL^{101}, at each HDX time from four glycoprofiles of AGP. Only doubly and triply charged peptides were subjected to ETD fragmentation, as we observed extensive hydrogen scrambling for quadruply charged peptide ions (data not shown). MagTran version 1.03 (Amgen, Thousand Oaks, CA)[29] was used to obtain the centroid of the deuterium-containing isotopic distribution for each product ion. The HDX–ETD experiments were performed on the glycopeptides in (at least) duplicate.

Peptide Identification and HDX Data Processing. Peptic peptides of AGP were identified using tandem MS (MS/MS) on the Thermo LTQ Orbitrap Elite instrument. One full mass spectral acquisition triggered six scans of MS/MS (precursor ion activated by CID) whereby the most abundant precursor ions were sequenced. Peptide identification was achieved by submitting Thermo RAW files to MASCOT (Matrix Science, Oxford, U.K.). The following MASCOT settings were used: enzyme, none; MS tolerance, 20 ppm; MS/MS tolerance, 0.6 Da; maximal number of missed cleavages, 3; and peptide charges, +1, +2, and +3. The centroid of each deuterated peptide spectrum envelope and the relative deuterium uptake of each peptide were calculated with HDX Workbench.[30] The most abundant glycan composition at each glycosite was used for HDX analysis of glycan-containing peptides (Table 1). Corrections of back exchange were made by considering the values of 80% deuterium content of the exchange buffer and 70% deuterium recovery based on the HDX results of maximally deuterated protein (HDX for 96 h at 37 °C). A paired t test between each pair of observed deuterium uptake data sets was computed with Prism version 5.01,[31] and the t test result identified statistically significant differences in the deuterium uptake between each glycoprofile pair. The quality of the data supported use of a $p < 0.05$ threshold for statistical significance.

RESULTS AND DISCUSSION

Glycosylation Profiles of AGP. AGP has five glycosites (Figure 1): N15, N38, N54, N75, and N85. Each of the N-glycosylation sites is occupied by complex-type N-linked glycans (bi-, tri-, and tetra-antennary branched, sialylated, and a trace fucosylated), resulting in a high degree of heterogeneity.[32] The glycoprofile of AGP has shown a high degree of diversity from study to study, particularly with respect to glycan chains missing in different environments.[3] Thus, it was crucial

dx.doi.org/10.1021/bi4011094 | *Biochemistry* 2013, 52, 7127–7136

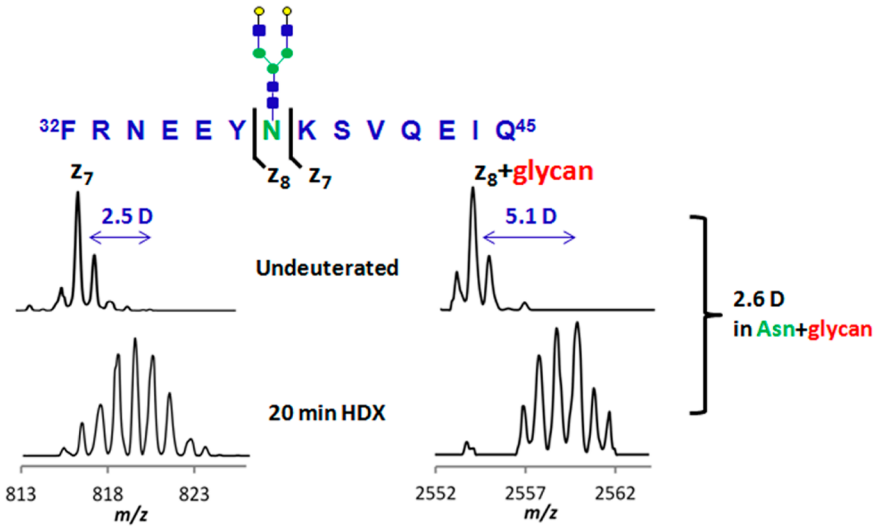

Figure 3. HDX–ETD of AGP glycopeptides. The deuterium retained in glycan groups in each HDX experiment was monitored by performing an ETD fragmentation strategy. ETD fragment ions (z_7 and z_8 ions) of triply charged glycopeptide FRENEEYNKSVQEIQ before and after HDX are shown.

for us to establish the glycoprofile of each AGP sample used in this study.

Treatment of native AGP with neuraminidase and fucosidase forms desialylated/defucosylated AGP. To separate the glycosidase-treated AGP from enzymes, digested AGP (and the native AGP) was purified by size exclusion chromatography (SEC), as described in Experimental Procedures (Figure S3A of the Supporting Information), and the retained product was analyzed by MALDI mass spectrometry (Figure S3B of the Supporting Information). Across the digested AGP samples, decreased glycoprotein masses were observed in the SEC data, and each diminished mass was verified by MALDI analysis. It is worth noting that the broadened parent ion peak of AGP observed in each MALDI spectrum indicates that a certain degree of heterogeneity among the glycoprofiles remains in each sample.

The glycan structures together with the extent of heterogeneity were identified via LC–MS/MS analysis. All samples were proteolyzed, and the glycopeptides from each sample were enriched and subjected to LC–MS/MS analysis (Experimental Procedures) (Figure S1 of the Supporting Information). Observation of oxonium ions of GlcNAc (m/z 204) that are generated in the ESI source indicated the presence of glycopeptides. Thus, the efficiency of glycopeptide enrichment was tested by comparing its total ion LC chromatogram profile to the extracted m/z 204 ion LC chromatogram profile from the corresponding crude proteolyzed AGP LC–MS/MS results (Figure S4 of the Supporting Information).[32] We observed a variety of glycan structures for each glycosite at a given LC retention time. The abundance of each glycan structure was then calculated using a label-free strategy as described in Experimental Procedures.

For the two AGP glycoprofiles, Figure 2 shows the fractional population of each glycostructure at each glycosite. The changes in glycan structures between desialylated/defucosylated AGP and native AGP (Figure 2, red vs blue) are consistent with the shift in elution times observed between these two samples on the SEC instrument (Figure S3A of the Supporting Information).

Native AGP exhibits a pattern of predominantly sialylated glycans that is in accord with the AGP glycoprofile reported previously[32] (Figure 2, blue bars). At glycosites I and II (Figure 2a,b), sialylated, diantennary complex-type oligosaccharides predominate. Glycosite III (Figure 2c) is predominately characterized by sialylated, tetra-antennary glycans and a trace [9 ± 1% (1σ)] of one partially sialylated, fucosylated, tetra-antennary glycan. At glycosite IV (Figure 2d), two sialylated, triantennary oligosaccharides predominate. At glycosite V (Figure 2e), one fully sialylated, tetra-antennary complex-type oligosaccharide predominates. Glyocosite V also has a trace [(≈5.4 ± 2.1)%] of the same tetra-antennary structure absent one NeuAc termination. Although eight glycan structures span the five glycosites, no more than four glycan structures are observed at any glycosite. Glycosite V is essentially homogeneous. At other glycosites, glycan structures largely differ by one NeuAc termination.

Following enzymatic treatment, the resulting desialylated/defucosylated AGP is predominately characterized by a restricted glycan distribution that contains no sialic acid or fucose groups (Figure 2, red bars). Glycosites I, IV, and V are predominately characterized by one oligosaccharide stoichiometry, and two oligosaccharide stoichiometries predominate at glycosites II and III.

The preparation of distinct, well-characterized glycoprofiles of AGP allowed us to use HDX–MS to measure variations in protein conformational dynamics induced by changes in glycan structures. In this study, the HDX measurements of each glycoprofile of AGP should provide the mean HDX behavior among different glycoforms within each glycoprofile. We have interpreted the HDX results of each glycoprofile according to its most abundant glycoform (Table 1). Given that we achieved complete removal of sialic acid from all glycan groups and the amount of fucose-attached glycan is negligible, we can examine the effects of desialylation on AGP biophysical properties in detail.

Ruling Out Digestion-Induced Conformational Changes in AGP. Measurements of peptide-level HDX kinetics have the potential to reveal protein dynamics in solution with a spatial resolution of 6–10 residues,[33] yet

dx.doi.org/10.1021/bi4011094 | Biochemistry 2013, 52, 7127–7136

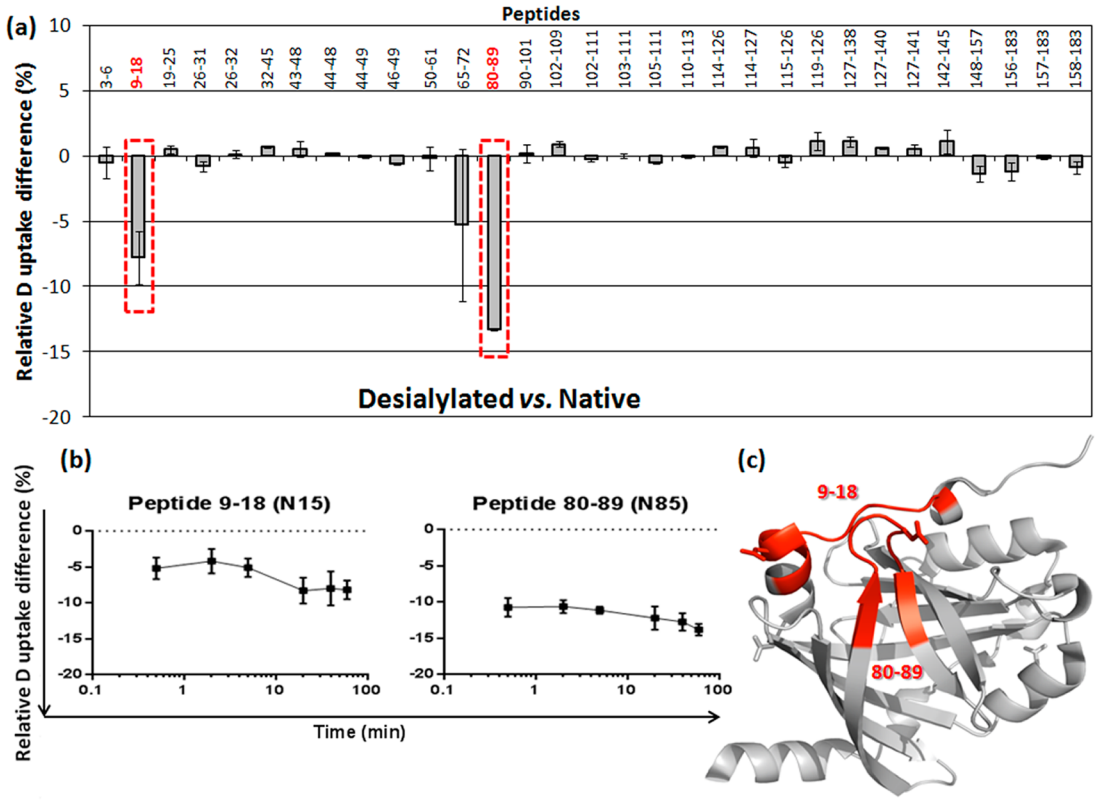

Figure 4. Differential HDX of peptides from AGP variants (desialylated vs native). (a) Average deuterium uptake differences (%) for six HDX time points of peptides identified in desialylated AGP relative to native AGP. Results are plotted with their standard deviations (1σ). Note the poor precision of HDX measurement of the region of residues 65−72. Regions (residues 9−18 and 80−89) that showed significant decreases in the level of uptake of deuterium upon desialylation are colored red. (b) Relative deuterium uptake differences (%) of peptide regions of residues 9−18 and 80−89 (desialylated vs native) plotted as a function of HDX time. Brackets denote the 1σ uncertainty. (c) Structural locations of peptide regions of residues 9−18 and 80−89 on the X-ray crystal structure of AGP (PDB entry 3KQ0).[1]

protein dynamics are sensitive to the conditions (pH, temperature, etc.) used during routine laboratory manipulations. A previous temperature-dependent study of AGP conformation via infrared spectroscopy showed no significant change in AGP conformation over a temperature range of 20−40 °C.[34] In this work, we observed nearly identical peptide-level HDX kinetics of native AGP before and after long-term incubation [(20 ± 2) h] in PBS buffer at 37 °C. The differential HDX map (Figure S5 of the Supporting Information) between unheated and heated native AGP exhibits average and maximal differences in D uptake (Δ%D) of (1 ± 1.4 (1σ))%D and −(4 ± 6)%D, respectively. Thus, the conformational dynamics of the native glycoprotein are unaffected by the heat treatment under this deglycosylation condition.

Another consideration is the possibility that treatment with the glycosidases will alter the higher-order structure. However, when we compare the two glycoprofiles, we observe no dramatic change in the H−D exchange rates among the AGP variants that can serve as evidence of deviation from the native structure. Instead, small, statistically significant changes are observed in relatively short regions (*vide infra*), indicating that the native structure is largely conserved during the deglycosylation process.

Measuring the Deuterium Retained on Glycan. HDX provides information about the deuterium uptake on protein backbone amides, which allows straightforward comparison of the protein physical properties in different environments. However, modifications of the protein side chain must be treated with caution especially when they contain exchangeable amide hydrogens. It has been observed previously[35] that the acetamido groups of GlcNAc and the side chain of modified Asn have the potential to retain measurable deuterium during the HDX−MS experiment. To avoid this source of systematic error, it is essential for us to measure the extent of deuterium uptake contributed by each glycan. A straightforward strategy for monitoring the extent of deuterium on glycans is to apply electron-transfer dissociation (ETD), electron-based gas-phase fragmentation methods, under conditions (Experimental Procedures) that prevent gas-phase hydrogen scrambling, on the deuterated peptides released upon proteolytic digestion.[36] The deuterium uptake of glycan-attached Asn was measured by the difference between a glycan-attached c_i or z_i ion and a $c_{(i-1)}$ or $z_{(i-1)}$ ion (Figure 3). The amounts of deuterium retained by the glycan chains and the attached Asn were determined for each HDX time point (Table S2 of the Supporting Information).

We observed that each pair of sialylated and desialylated glycopeptides share a similar LC retention time (Table 1), mandating that the extent of back-exchange for each pair be nearly the same. We also observed a similar amount of deuterium uptake by glycan-attached Asn for both sialylated and desialylated glycopeptides (Table S2 of the Supporting Information). The observations support our conclusion that the uptake of deuterium by glycans has little effect on the differential HDX measurements.

dx.doi.org/10.1021/bi4011094 | *Biochemistry* 2013, 52, 7127−7136

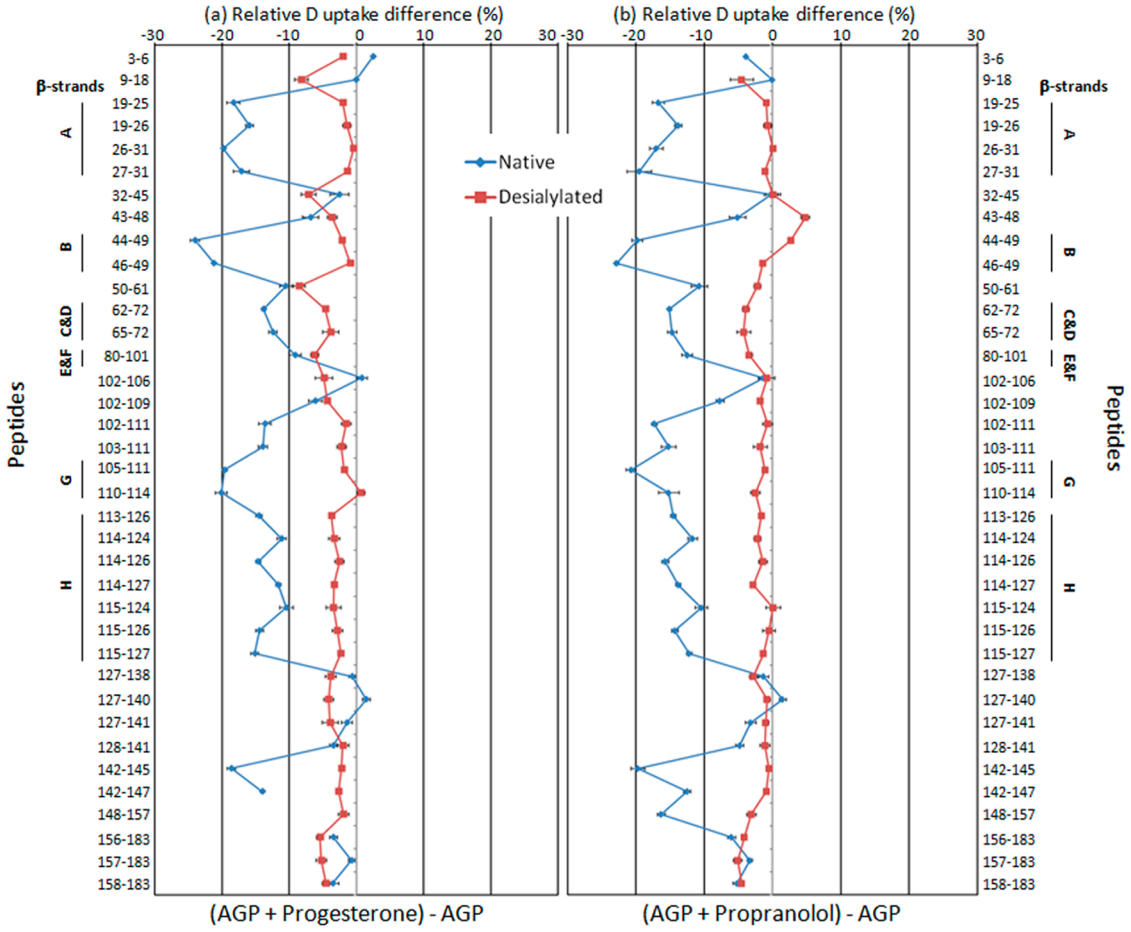

Figure 5. Relative D uptake differences between ligand-bound AGP and ligand-free AGP. The average relative D uptake differences of peptic peptides for six HDX time points from native AGP (blue) and desialylated AGP (red) with respect to progesterone binding (a) and propranolol binding (b) are plotted together with their standard deviations (1σ). The locations of eight β-strands that form the ligand-binding cavity are labeled.

Desialylation Induces Conformational Changes in AGP. Figure 4a shows the average deuterium uptake differences (%) by all peptides observed in desialylated/defucosylated AGP relative to native AGP. It was shown previously that the intensities of glycopeptide ions in mass spectrometry are easily suppressed by unglycosylated peptide ions in positive ion mode and that this suppression leads to a lower level of sequence coverage.[32] This effect likely accounts for the absence of data for residue 73−79 (IYNTTYL) and reduces the level of sequence coverage from 97% (Figure S6 of the Supporting Information) to 91%.

These HDX results show that the removal of sialic acid from native AGP has a significant impact on peptide regions containing N85 glycosites (residues 80−89; p = 0.001 from t test, where $p < 0.05$ is significant) and a minor impact on peptide regions containing N15 glycosites (residues 9−18; p = 0.03) (Figure 4a,b). Several amides in these two regions underwent relatively rapid deuterium uptake in sialylated AGP, whereas in unsialylated AGP, these same amides exchanged deuterium more slowly. We observed a similar trend of HDX for the less abundant glycoforms in these two regions (data not shown). Therefore, this phenomenon may not be glycoform-specific; that is, addition of sialic acid to the glycan structures makes both regions more structurally labile to hydrogen exchange. Interestingly, these two regions are geometrically close to each other, and both are located outside of the ligand-binding cavity[4] (Figure 4c).

Previous studies of the effects of sialylation on the immunomodulatory functions of AGP have shown that an inflammation-induced increase in the level of sialylation of AGP inhibits the extravasation of granulocytes.[37] Furthermore, desialylation of AGP can inhibit the aggregation of platelets in blood and affect AGP drug binding.[9,10] The change in conformational dynamics in these regions, as observed in our study, may play a role during immune responses.

Effects of Desialylation on AGP−Ligand Interactions. Previous studies of AGP−ligand interactions show that Trp122 and Tyr127 in β-strand H and Trp25 in β-strand B of AGP interact with progesterone and propranolol through hydrogen bonds, as revealed by Raman difference spectroscopy and computer docking,[1,4] circular dichroism,[38] and fluorescence measurement.[39] The association constants between progesterone and AGP and between propranolol and AGP are in the range of 10^5 L mol^{-1},[40] and the stoichiometries between progesterone and AGP and between propranolol and AGP are approximately 1.[40] Previous measurements found that desialylation reduces the binding affinity of propranolol for AGP by 1.4-fold. In contrast, the affinity of progesterone is not affected.[40]

We prepared samples under conditions that can form stable AGP−ligand complexes (Experimental Procedures). Figure 5 shows the relative D uptake differences among peptic peptides of native AGP (Figure 5, blue) and desialylated AGP (Figure 5, red) with respect to progesterone (Figure 5a) and propranolol

dx.doi.org/10.1021/bi4011094 | Biochemistry 2013, 52, 7127−7136

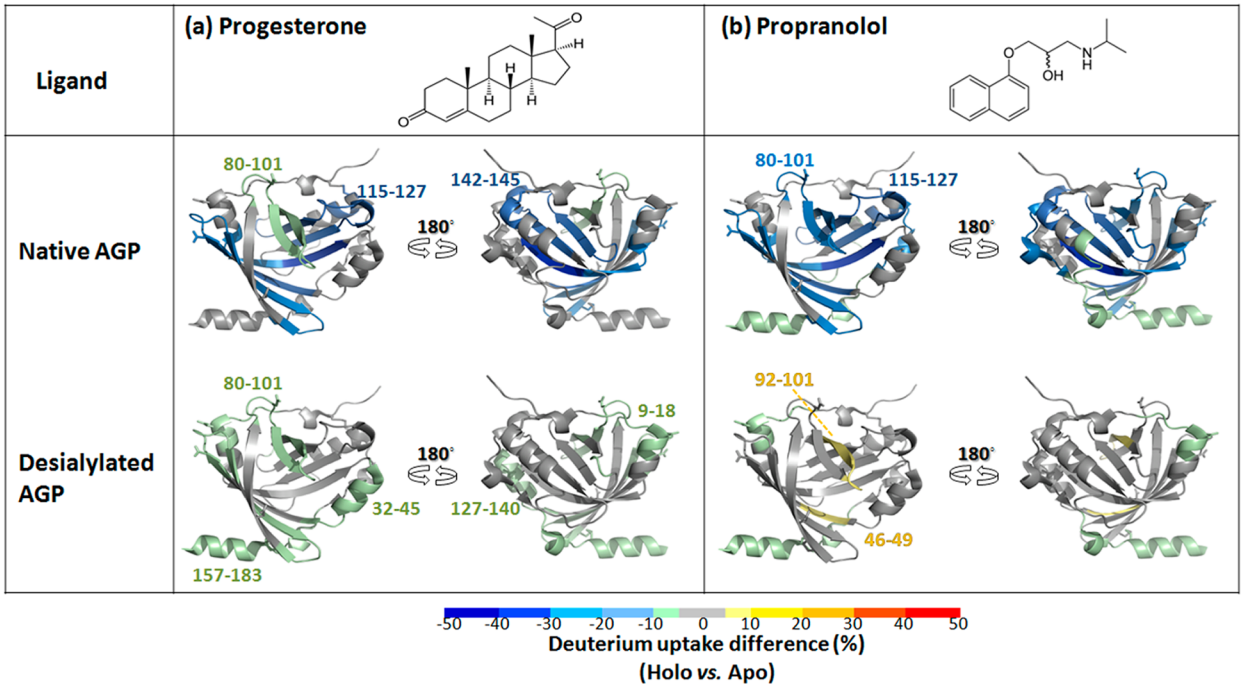

Figure 6. Structural locations of AGP peptide regions exhibiting significant changes in conformational dynamics upon ligand binding. Average deuterium uptake differences (%) for six HDX time points of peptides identified in native AGP (top) and desialylated AGP (bottom) upon progesterone (a) and propranolol (b) binding are mapped on the X-ray crystal structure of AGP (PDB entry 3KQ0).[1] The extent of D uptake difference from negative to positive is presented with color ranging from blue to red. Brackets denote the 1σ standard deviation.

bindings (Figure 5b). Not surprisingly, all eight β-strands, comprising the AGP ligand-binding cavity, show significant decreases in the levels of deuterium uptake upon progesterone and propranolol binding. This suggests the β-sheet barrel of AGP that forms the ligand-binding cavity is structurally stabilized upon ligand binding (Figure 6).

The removal of sialic acid dramatically diminished the conformational changes of AGP upon binding with progesterone or propranolol (Figure 5, red vs blue), suggesting weaker interactions among AGP and the ligands. This phenomenon observed in the HDX–MS results is more obvious for propranolol binding, and it is in accord with a previous finding that the binding affinity of propranolol for AGP becomes significantly diminished upon desialylation.[40] Interestingly, our HDX results show peptide regions of residues 46–49 and 92–101 of desialylated AGP, a part of the ligand-binding cavity, become more structurally labile compared to native AGP upon propranolol binding (Figure 6b, bottom, yellow).

For progesterone binding, several helix–loop regions in desialylated AGP, including the entrance of the AGP ligand-binding cavity[1] (residues 32–45) and residues 9–18, a region that becomes structurally stable upon desialylation (Figure 4), showed slightly more protection upon progesterone binding than native AGP (Figure 6a, bottom). This suggests progesterone binds to desialylated AGP through an altered mechanism compared to that of native AGP.

In summary, application of HDX–MS reveals that the removal of sialic acids structurally stabilizes two regions (residues 9–18 and 80–89) that are exterior to the β-sheet barrel of AGP. This structural stabilization further affects ligand binding-induced conformational changes of AGP and, therefore, may be the key factor in regulating the ligand-binding properties of AGP.

CONCLUSIONS

HDX–MS is recognized as a powerful technique that measures the dynamical structure of glycoproteins. The method has no known upper mass limit, and it can provide information about protein dynamic that are difficult to achieve by other analytical strategies such as NMR and X-ray crystallography. In our study, we utilized the advantages of this technique to reveal, for the first time, the effects of desialylation on the conformational dynamics of AGP and AGP–ligand binding at high resolution.

Our MS-based approach combined with HDX not only identified the glycoprofile of AGP, which has a mixture of di-, tri-, and tetra-antennary complex-type N-linked glycan groups, but also revealed the effects of desialylation on AGP–ligand interaction from a structural point of view.

The regions of AGP that showed differential HDX between native and desialylated AGP include residues in two regions (residues 9–18 and 80–89), which are located outside of the AGP ligand-binding cavity. The conformational changes of these two regions further regulate the ligand binding activities of AGP. A future study that applies site-specific desialylation should be able to pinpoint the glycan sites that are involved in regulating these processes.

ASSOCIATED CONTENT

Supporting Information

Supplemental figures. This material is available free of charge via the Internet at http://pubs.acs.org.

AUTHOR INFORMATION

Corresponding Author

*E-mail: jeffrey.hudgens@nist.gov. Telephone: (240) 314-6485. Fax: (240) 314-6255.

Funding

R.Y.-C.H. acknowledges the support of a National Academy of Science's National Research Council postdoctoral fellowship.

Notes

The authors declare no competing financial interest.

■ ACKNOWLEDGMENTS

We thank Dr. Todd Hoopes in the Biomolecular Labeling Laboratory (Institute for Bioscience and Biotechnology Research) for assistance with size exclusion chromatography.

■ ABBREVIATIONS

ESI, electrospray ionization; MS, mass spectrometry; FTMS, Fourier transform mass spectrometry; CID, collision-induced dissociation; HDX, hydrogen−deuterium exchange; ETD, electron-transfer dissociation; NeuAc, *N*-acetylneuraminic acid; Hex, hexose; GlcNAc, *N*-acetylglucosamine; AGP, human α1-acid glycoprotein; PDB, Protein Data Bank.

■ REFERENCES

(1) Schönfeld, D. L., Ravelli, R. B. G., Mueller, U., and Skerra, A. (2008) The 1.8-Å Crystal Structure of α1-Acid Glycoprotein (Orosomucoid) Solved by UV RIP Reveals the Broad Drug-Binding Activity of This Human Plasma Lipocalin. *J. Mol. Biol. 384*, 393−405.

(2) Schmid, K., Buergi, W., Collins, J. H., and Nanno, S. (1974) Disulfide bonds of α1-acid glycoprotein. *Biochemistry 13*, 2694−2697.

(3) Shiyan, S. D., and Bovin, N. V. (1997) Carbohydrate composition and immunomodulatory activity of different glycoforms of α1-acid glycoprotein. *Glycoconjugate J. 14*, 631−638.

(4) Kopecký, V. R., Jr., Ettrich, R., Hofbauerová, K., and Baumruk, V. R. (2003) Structure of human α1-acid glycoprotein and its high-affinity binding site. *Biochem. Biophys. Res. 300*, 41−46.

(5) Israili, Z., and Dayton, P. (2001) Human α1-Glycoprotein and Its Interactions with Drugs. *Drug Metab. Rev. 33*, 161.

(6) Bennett, M., and Schmid, K. (1980) Immunosuppression by human plasma α1-acid glycoprotein: Importance of the carbohydrate moiety. *Proc. Natl. Acad. Sci. U.S.A. 77*, 6109−6113.

(7) Dente, L., Rüther, U., Tripodi, M., Wagner, E. F., and Cortese, R. (1988) Expression of human α1-acid glycoprotein genes in cultured cells and in transgenic mice. *Genes Dev. 2*, 259−266.

(8) Kishino, S., Nomura, A., Saitoh, M., Sugawara, M., Iseki, K., Kitabatake, A., and Miyazaki, K. (1997) Single-step isolation method for six glycoforms of human α1-acid glycoprotein by hydroxylapatite chromatography and study of their binding capacities for disopyramide. *J. Chromatogr., B: Anal. Technol. Biomed. Life Sci. 703*, 1−6.

(9) Fournier, T., Medjoubi-N, N., and Porquet, D. (2000) α1-Acid glycoprotein. *Biochim. Biophys. Acta 1482*, 157−171.

(10) Costello, M., Fiedel, B. A., and Gewurz, H. (1979) Inhibition of platelet aggregation by native and desialised α1 acid glycoprotein. *Nature 281*, 677−678.

(11) Chalmers, M. J., Busby, S. A., Pascal, B. D., West, G. M., and Griffin, P. R. (2011) Differential hydrogen/deuterium exchange mass spectrometry analysis of protein-ligand interactions. *Expert Rev. Proteomics 8*, 43−59.

(12) Engen, J. R. (2009) Analysis of Protein Conformation and Dynamics by Hydrogen/Deuterium Exchange MS. *Anal. Chem. 81*, 7870−7875.

(13) Huang, R. Y. C., Wen, J., Blankenship, R. E., and Gross, M. L. (2012) Hydrogen−Deuterium Exchange Mass Spectrometry Reveals the Interaction of Fenna−Matthews−Olson Protein and Chlorosome CsmA Protein. *Biochemistry 51*, 187−193.

(14) Pan, J., Han, J., Borchers, C. H., and Konermann, L. (2011) Conformer-Specific Hydrogen Exchange Analysis of Aβ(1−42) Oligomers by Top-Down Electron Capture Dissociation Mass Spectrometry. *Anal. Chem. 83*, 5386−5393.

(15) Thompson, N. J., Rosati, S., Rose, R. J., and Heck, A. J. R. (2013) The impact of mass spectrometry on the study of intact antibodies: From post-translational modifications to structural analysis. *Chem. Commun. 49*, 538−548.

(16) Wang, L., Pan, H., and Smith, D. L. (2002) Hydrogen Exchange-Mass Spectrometry. *Mol. Cell. Proteomics 1*, 132−138.

(17) Skinner, J. J., Lim, W. K., Bédard, S., Black, B. E., and Englander, S. W. (2012) Protein dynamics viewed by hydrogen exchange. *Protein Sci. 21*, 996−1005.

(18) Truhlar, S. E., Croy, C., Torpey, J., Koeppe, J., and Komives, E. (2006) Solvent accessibility of protein surfaces by amide H/^{2}H exchange MALDI-TOF mass spectrometry. *J. Am. Soc. Mass Spectrom. 17*, 1490−1497.

(19) Joao, H. C., Scragg, I. G., and Dwek, R. A. (1992) Effects of glycosylation on protein conformation and amide proton exchange rates in RNase B. *FEBS Lett. 307*, 343−346.

(20) De Beer, T., Van Zuylen, C. W. E. M., Leeflang, B. R., Hård, K., Boelens, R., Kaptein, R., Kamerling, J. P., and Vliegenthart, J. F. G. (1996) NMR Studies of the Free α Subunit of Human Chorionic Gonadotropin. *Eur. J. Biochem. 241*, 229−242.

(21) Houde, D., Arndt, J., Domeier, W., Berkowitz, S., and Engen, J. R. (2009) Characterization of IgG1 Conformation and Conformational Dynamics by Hydrogen/Deuterium Exchange Mass Spectrometry. *Anal. Chem. 81*, 5966−5966.

(22) Houde, D., Peng, Y., Berkowitz, S. A., and Engen, J. R. (2010) Post-translational Modifications Differentially Affect IgG1 Conformation and Receptor Binding. *Mol. Cell. Proteomics 9*, 1716−1728.

(23) Sarkar, A., and Wintrode, P. L. (2011) Effects of glycosylation on the stability and flexibility of a metastable protein: The human serpin α1-antitrypsin. *Int. J. Mass Spectrom. 302*, 69−75.

(24) Busby, S. A., Chalmers, M. J., and Griffin, P. R. (2007) Improving digestion efficiency under H/D exchange conditions with activated pepsinogen coupled columns. *Int. J. Mass Spectrom. 259*, 130−139.

(25) Xu, H., and Freitas, M. A. (2009) MassMatrix: A database search program for rapid characterization of proteins and peptides from tandem mass spectrometry data. *Proteomics 9*, 1548−1555.

(26) Xu, H., Zhang, L., and Freitas, M. A. (2008) Identification and Characterization of Disulfide Bonds in Proteins and Peptides from Tandem MS Data by Use of the MassMatrix MS/MS Search Engine. *J. Proteome Res. 7*, 138−144.

(27) Burns, K. M., Rey, M., Baker, C. A. H., and Schriemer, D. C. (2013) Platform Dependencies in Bottom-up Hydrogen/Deuterium Exchange Mass Spectrometry. *Mol. Cell. Proteomics 12*, 539−548.

(28) Zehl, M., Rand, K. D., Jensen, O. N., and Jorgensen, T. J. D. (2008) Electron Transfer Dissociation Facilitates the Measurement of Deuterium Incorporation into Selectively Labeled Peptides with Single Residue Resolution. *J. Am. Chem. Soc. 130*, 17453−17459.

(29) Zhang, Z., and Marshall, A. (1998) A universal algorithm for fast and automated charge state deconvolution of electrospray mass-to-charge ratio spectra. *J. Am. Soc. Mass Spectrom. 9*, 225−233.

(30) Pascal, B., Willis, S., Lauer, J., Landgraf, R., West, G., Marciano, D., Novick, S., Goswami, D., Chalmers, M., and Griffin, P. (2012) HDX Workbench: Software for the Analysis of H/D Exchange MS Data. *J. Am. Soc. Mass Spectrom. 23*, 1512−1521.

(31) Press, W. H., Teukolsky, S. A., Vetterling, W. T., and Flannery, B. P. (2007) Numerical Recipes. *The Art of Scientific Computing*, 3rd ed., Cambridge University Press, Cambridge, U.K.

(32) Imre, T., Schlosser, G., Pocsfalvi, G., Siciliano, R., Molnár-Szöllősi, É., Kremmer, T., Malorni, A., and Vékey, K. (2005) Glycosylation site analysis of human α1-acid glycoprotein (AGP) by capillary liquid chromatography—electrospray mass spectrometry. *J. Mass Spectrom. 40*, 1472−1483.

(33) Rand, K. D., Zehl, M., Jensen, O. N., and Jorgensen, T. J. D. (2009) Protein Hydrogen Exchange Measured at Single-Residue Resolution by Electron Transfer Dissociation Mass Spectrometry. *Anal. Chem. 81*, 5577−5584.

(34) Ausili, A., Scirè, A., Damiani, E., Zolese, G., Bertoli, E., and Tanfani, F. (2005) Temperature-Induced Molten Globule-like State in

Human α1-Acid Glycoprotein: An Infrared Spectroscopic Study. *Biochemistry 44*, 15997−16006.
(35) Guttman, M., Scian, M., and Lee, K. K. (2011) Tracking Hydrogen/Deuterium Exchange at Glycan Sites in Glycoproteins by Mass Spectrometry. *Anal. Chem. 83*, 7492−7499.
(36) Hassell, K. M., Guttman, M., Lee, K., and Engen, J. R. (2012) Hydrogen Exchange Mass Spectrometry Coupled with ETD to Study Glycan Amide Exchange Properties, In American Society for Mass Spectrometry, Vancouver.
(37) Boutten, A., Dehoux, M., Deschenes, M., Rouzeau, J.-D., Bories, P. N., and Durand, G. (1992) α1-Acid glycoprotein potentiates lipopolysaccharide-induced secretion of interleukin-1 β, interleukin-6 and tumor necrosis factor-α by human monocytes and alveolar and peritoneal macrophages. *Eur. J. Immunol. 22*, 2687−2695.
(38) Zsila, F., and Iwao, Y. (2007) The drug binding site of human α1-acid glycoprotein: Insight from induced circular dichroism and electronic absorption spectra. *Biochim. Biophys. Acta 1770*, 797−809.
(39) Albani, J. R. (2006) Progesterone binding to the tryptophan residues of human α1-acid glycoprotein. *Carbohydr. Res. 341*, 2557−2564.
(40) Wang, A. K. L., and Hsia, J. C. (1983) In vitro binding of propranolol and progesterone to native and desialylated human orosomucoid. *Can. J. Biochem. Cell Biol. 61*, 1114−1116.